Article

Cell Metabolism

Celastrol Protects against Obesity and Metabolic Dysfunction through Activation of a HSF1-PGC1α Transcriptional Axis

Graphical Abstract

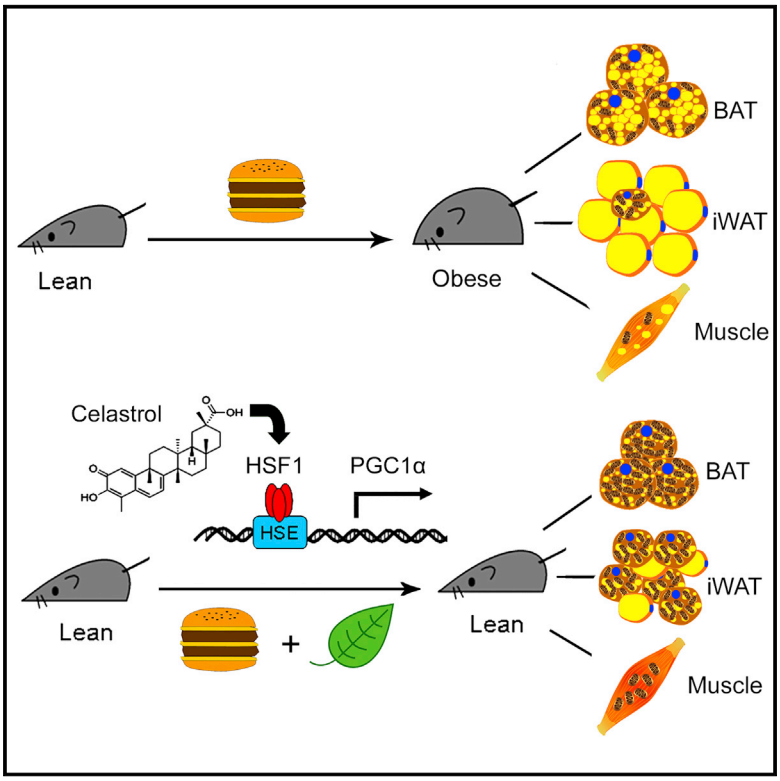

Highlights

- HSF1 regulates PGC1α-dependent metabolic programs in adipose tissues and muscle
- Celastrol increases mitochondrial function in fat and muscle via HSF1
- Celastrol enhances energy expenditure and protects mice on HFD from developing obesity
- Celastrol increases muscle endurance

Authors

Xinran Ma, Lingyan Xu, Anna Teresa Alberobello, ..., Jie Liu, Toren Finkel, Elisabetta Mueller

Correspondence

elisabettam@niddk.nih.gov

In Brief

Ma et al. identify the cellular thermal sensor HSF1 as an upstream activator of PGC1α. The natural compound celastrol activates HSF1 and protects against obesity and metabolic dysfunction by increasing energy expenditure, inducing iWAT browning, BAT activation, and mitochondrial genes in muscle.

Ma et al., 2015, Cell Metabolism 22, 695–708
October 6, 2015
http://dx.doi.org/10.1016/j.cmet.2015.08.005

Cell Metabolism
Article

Celastrol Protects against Obesity and Metabolic Dysfunction through Activation of a HSF1-PGC1α Transcriptional Axis

Xinran Ma,[1,5] Lingyan Xu,[1,5] Anna Teresa Alberobello,[1] Oksana Gavrilova,[2] Alessia Bagattin,[1] Monica Skarulis,[3] Jie Liu,[4] Toren Finkel,[4] and Elisabetta Mueller[1,*]
[1]Genetics of Development and Disease Branch, National Institute of Diabetes and Digestive and Kidney Diseases, National Institutes of Health, Bethesda, MD 20892, USA
[2]Mouse Metabolism Core, National Institute of Diabetes and Digestive and Kidney Diseases, National Institutes of Health, Bethesda, MD 20892, USA
[3]Clinical Endocrine Section, National Institute of Diabetes and Digestive and Kidney Diseases, National Institutes of Health, Bethesda, MD 20892, USA
[4]Center for Molecular Medicine, National Heart, Lung, and Blood Institute, National Institutes of Health, Bethesda, MD 20892, USA
[5]Co-first author
*Correspondence: elisabettam@niddk.nih.gov
http://dx.doi.org/10.1016/j.cmet.2015.08.005

SUMMARY

Altering the balance between energy intake and expenditure is a potential strategy for treating obesity and metabolic syndrome. Nonetheless, despite years of progress in identifying diverse molecular targets, biological-based therapies are limited. Here we demonstrate that heat shock factor 1 (HSF1) regulates energy expenditure through activation of a PGC1α-dependent metabolic program in adipose tissues and muscle. Genetic modulation of HSF1 levels altered white fat remodeling and thermogenesis, and pharmacological activation of HSF1 via celastrol was associated with enhanced energy expenditure, increased mitochondrial function in fat and muscle and protection against obesity, insulin resistance, and hepatic steatosis during high-fat diet regimens. The beneficial metabolic changes elicited by celastrol were abrogated in HSF1 knockout mice. Overall, our findings identify the temperature sensor HSF1 as a regulator of energy metabolism and demonstrate that augmenting HSF1 via celastrol represents a possible therapeutic strategy to treat obesity and its myriad metabolic consequences.

INTRODUCTION

The accumulation of excessive fat tissue, the result of an imbalance between energy input and its output, leads to obesity, diabetes, cardiovascular disease, and hepatosteatosis, which together represent the leading causes of adult morbidity and mortality worldwide. The main site of energy storage is white adipose tissue (Farmer, 2008; Mueller, 2014; Gesta et al., 2007), while brown fat is principally involved in energy expenditure via thermogenesis, achieved through the dissipation of chemical energy via the activity of Uncoupling Protein 1 (UCP1), a mitochondrial protein uncoupling respiration from ATP synthesis. For a considerable period of time this rigid framework defined our view of how energy balance was controlled. Recently, this viewpoint has been altered to incorporate the observation that adult humans contain measurable amounts of brown fat (Cypess et al., 2009; Skarulis et al., 2010; Ouellet et al., 2012). Recently a new cell type of smooth muscle origin (Long et al., 2014), called brite or beige, has been shown to be inducible upon cold or hormonal stimuli, causing brown remodeling of white fat, expressing UCP1 and contributing to energy expenditure (Nedergaard and Cannon, 2014; Wu et al., 2012; Sharp et al., 2012). In addition, beige cells directly sense temperature changes, suggesting a cell-autonomous mechanism to activate thermogenesis in brite/beige fat depots (Ye et al., 2013). This newly discovered "plasticity" of adipocytes has intensified efforts to identify novel methods to treat obesity and insulin resistance by increasing browning and peripheral energy expenditure (Boss and Farmer, 2012; Cypess and Kahn, 2010).

Mitochondrial dysfunction has been shown to be associated with the development of obesity and insulin resistance (Bournat and Brown, 2010; Patti and Corvera, 2010). The peroxisome proliferator-activated receptor γ coactivator-1α (PGC-1α) is a central transcriptional regulator of mitochondrial and peroxisomal remodeling and biogenesis (Wu et al., 1999; Bagattin et al., 2010). Genetic analysis of PGC1α requirement in vivo via generation of total and conditional knockout mice has revealed its involvement in thermogenesis, mitochondrial gene expression (Lin et al., 2004; Leone et al., 2005), and browning of white fat tissues (Kleiner et al., 2012). In addition to fat, skeletal muscle represents a critical metabolic organ in energy homeostasis. It has been shown that PGC1α controls mitochondrial and oxidative fiber conversion gene programs in muscle to increase energy expenditure to match metabolic needs (Handschin and Spiegelman, 2006; Lagouge et al., 2006). Interestingly, mice with neuronal inactivation of PGC1α show hyperactivity and resistance to diet-induced obesity but normal adaptive response to cold exposure, suggesting critical metabolic roles of PGC1α in both central and peripheral tissues (Ma et al., 2010). PGC1α is tightly regulated by a number of signal transduction effectors,

such as AMPK, SIRT1, mTOR, and GCN5, which orchestrate posttranslational modifications that either enhance or repress PGC1α activity in brown adipose tissue, muscle, and liver (Cantó and Auwerx, 2009; Cunningham et al., 2007; Lerin et al., 2006) and transcriptionally induced by thermal, oxidative, and mechanical challenges (St-Pierre et al., 2006; Handschin et al., 2007; Egan et al., 2010).

In response to stress, activated heat shock factor 1 (HSF1) exerts pleotropic effects (Anckar and Sistonen, 2011). In addition to the classic induction by heat shock, HSF1 is also activated by cold temperatures (Cullen and Sarge, 1997) and plays a role in circadian changes in body temperature through clock gene regulation (Reinke et al., 2008). To date, there has been no mechanistic link between HSF1 and PGC1α, although a recent genome-wide analysis of PGC1α binding sites in transformed hepatocytes raised the possibility of potential occupancy of PGC1α at heat shock response elements in liver cells (Charos et al., 2012). HSF1's most explored function to date has been the regulation of the expression of genes encoding for chaperone proteins to protect cells against temperature changes, oxidative stress, and hypoxia. In response to these stimuli, HSF1 is activated via the dissociation of HSP90, HSP70, and HSP40, and, upon multimerization and posttranslational modifications (Xu et al., 2012), HSF1 binds to DNA to induce its downstream gene targets through three types of heat shock elements (HSEs). These elements are defined depending on the organization of their GAA/TTC core domains as classic, gap type, or TTC rich (Eastmond and Nelson, 2006; Guo et al., 2008). HSF1 activity can be modulated by a variety of compounds with different chemical structures (Fujikake et al., 2008). One such agent is celastrol, a compound that is known to be capable of inducing classic HSF1 heat shock target genes (Westerheide et al., 2004). Despite the number of reports on the biological functions of HSF1, no studies have yet specifically evaluated the effects of modulation of HSF1 levels and activity on energy metabolism. Here, we directly linked the activation of HSF1 to the induction of PGC1α gene expression and to that of PGC1α downstream programs, thereby defining a critical regulatory axis between these two transcription factors. We show that activation of HSF1 by the natural compound celastrol has profound effects in vitro and in vivo in mice on high-fat diet (HFD) by increasing their energy expenditure, inducing browning of iWAT and brown fat programs in BAT, and activating mitochondrial gene targets in muscle. Our work identifies HSF1 as an important metabolic regulator in mesenchymal cells and tissues and proposes a potent pathway that can be activated for the treatment of obesity and related metabolic disorders.

RESULTS

HSF1 Regulates PGC1α Levels and Brown and Mitochondrial Gene Programs In Vitro

Given the established role of PGC1α in browning of white fat tissue (Wu et al., 1999, Kleiner et al., 2012) and in increasing mitochondrial function in muscle (Lin et al., 2002), we aimed to identify upstream regulators of PGC1α and used the transcriptional activation of PGC1α as a readout to characterize novel regulators of energy expenditure. By performing an in silico screen of transcription factor binding elements in the regulatory region upstream of the *PGC1α* start site, we identified multiple repeats exhibiting the characteristic core motif 5′-nTTCn-3′ (see Figure S1A available online), previously described as a non-canonical TTC-rich binding site for the heat shock transcription factor HSF1 (Eastmond and Nelson, 2006; Guo et al., 2008). Electromobility shift analysis and luciferase reporter assays confirmed HSF1's binding at nucleotides −2,369 to −2,346 in the mouse *PGC1α* promoter (Figures 1A and S1B). To determine the physiological relevance of this finding, we performed chromatin immunoprecipitation (ChIP) assays and showed increased HSF1 occupancy at this site, but not at control sites, in BAT and iWAT of mice exposed to cold temperatures (Figures 1B and S1C). Given the previously reported role of PGC1α in the potentiation of its own expression (Handschin et al., 2003), we next performed coimmunoprecipitation studies to assess the interaction between PGC1α and HSF1 on the PGC1α promoter. Our analysis revealed that HSF1 binds to PGC1α and that this interaction is enhanced by the addition of the HSF1 activator celastrol (Figure 1C). Furthermore, ChIP and re-ChIP studies confirmed that PGC1α and HSF1 co-occupy selectively the HSE in the PGC1α promoter (Figures 1D, S1D, and S1E).

We next used the mesenchymal cell line 10T1/2, previously shown to induce endogenous *PGC1α* levels in response to a variety of stimuli (St-Pierre et al., 2006), to test the effects of HSF1 modulation in vitro. Forced HSF1 expression increased *PGC1α* mRNA levels, which were further elevated after the addition of celastrol (Figure S1F). The ability of HSF1 to induce *PGC1α* mRNA was also confirmed using additional activators of HSF1 (Fujikake et al., 2008), such as the chemical compounds 17-allylamino-17-demethoxy-geldanamycin (17-AAG), geranylgeranylacetone (GAA), or radicicol (RA) and through classic heat shock stimulation (Figure S1G). These results indicated that *PGC1α* levels are indeed elevated as a result of HSF1 activation, rather than the consequence of nonspecific, off-target effects of selected compounds. Analysis of isoform selectivity revealed that *PGC1α1* is the only *PGC* family member regulated by HSF1 and that there are no compensatory changes in *PGC1β* (Figure S1H). Further analysis of HSF1's activation revealed the elevation of brown fat selective markers, such as *PRDM16* and *UCP1*, as well as mitochondrial and fatty acid metabolism genes (Figures 1E and S1I–1L), but no induction of differentiation genes (Figure S1M). The heat shock protein *HSP70*, an established gene target of HSF1, served as a marker for the efficacy of the activators used to elicit HSF1-mediated transcriptional responses.

Given the presence of a HSE in the upstream regulatory regions of the human *PGC1α* gene (Figure S1A), we tested the effects of HSF1 activation in cells obtained from subcutaneous fat of obese patients. Similarly to murine cells, brown-specific gene expression programs were increased by celastrol in differentiated stromal-vascular fraction (SVF) cells obtained from obese subjects, thereby confirming the role of HSF1 in the regulation of *PGC1α* and brown fat and mitochondrial programs in human cells as well (Figure S1N). Furthermore, ablation of *HSF1* function via HSF1 siRNA knockdown reduced the expression levels of *PGC1α* and that of its target genes, further confirming that HSF1 regulates *PGC1α* and brown fat markers (Figures 1F and S1O).

Given that HSF1 binds to the *PGC1α* promoter after acute cold exposure (Figure 1B) and the previously reported evidence

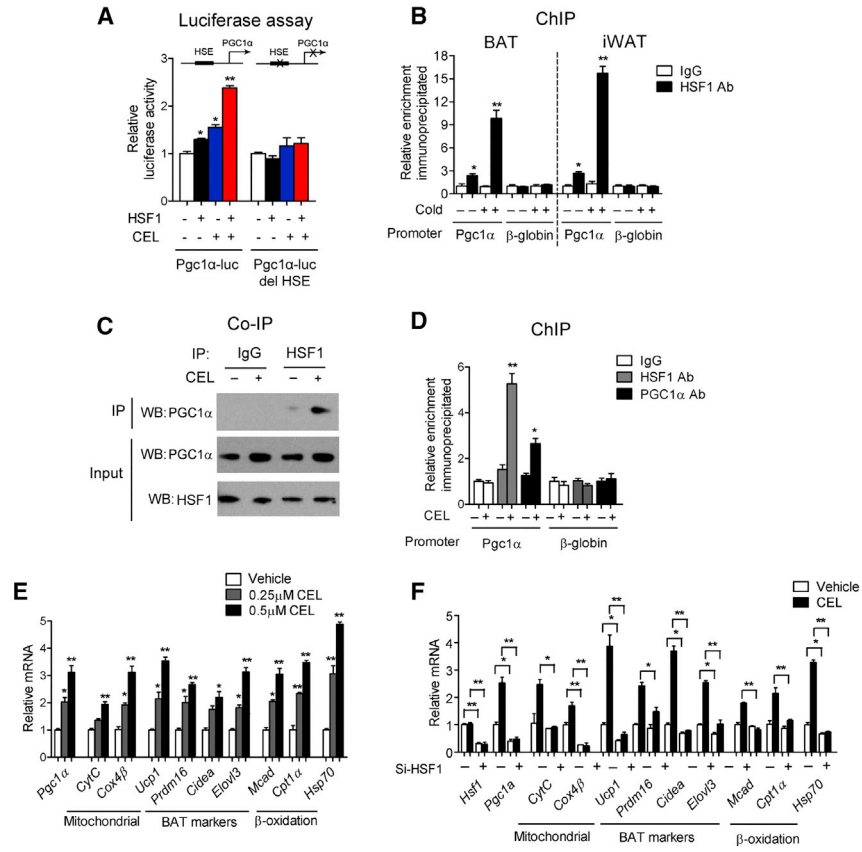

Figure 1. HSF1 Regulates PGC1α and PGC1α-Dependent Gene Programs

(A) HSF1 overexpression and its activation by celastrol (CEL) in 10T1/2 cells induce a luciferase wild-type *PGC1α* promoter reporter (PGC1α-luc), but not a mutant reporter with a deletion of the putative HSE site (PGC1α-luc del HSE).

(B) In vivo ChIP assay assessing HSF1 binding at the putative HSE site in the *PGC1α* promoter or in the β-globin promoter in BAT and iWAT of mice exposed to room temperature or to cold for 2 hr.

(C) CoIP analysis of HSF1 and PGC1α interaction in differentiated 10T1/2 cells with or without CEL treatment.

(D) ChIP assay in 10T1/2 cells assessing HSF1 and PGC1α occupancy at the putative HSE site in the *PGC1α* promoter and at the β-globin promoter, in the presence (+) or absence (−) of CEL.

(E) Regulation of *PGC1α* and brown fat gene levels by CEL in differentiated 10T1/2 cells.

(F) Analysis of the levels of *PGC1α* mRNAs in control and in HSF1 knockdown (Si-HSF1) differentiated 10T1/2 cells treated with vehicle or CEL.

Data are presented as mean ± SEM from three independent experiments and $^{*}p < 0.05$, $^{**}p < 0.01$ compared to control group.

of fat cells' intrinsic capability to sense cold temperatures, we assessed the potential involvement of HSF1 in cell-autonomous cold sensing. We exposed control or HSF1 siRNA expressing cells to 31°C, a temperature known to induce the expression of UCP1 in isolated cells (Ye et al., 2013), and demonstrated that while control cells responded to cooling by increasing *PGC1α* and *UCP1* levels, cells with HSF1 knockdown had a blunted induction of these thermogenic factors (Figures S1P–S1R). These data suggest a potential role for HSF1 in fat-cell-autonomous temperature sensing and in eliciting thermogenic responses.

HSF1 Null Mice Have Impaired Energy Metabolism

Based on the observation that HSF1 regulates the expression of brown fat markers and mitochondrial genes in vitro (Figure 1), we next performed genetic analyses to determine whether modulation of HSF1 levels in vivo would alter metabolism. Given that no studies to date have assessed the impact of HSF1 on energy balance, we characterized the metabolic consequences of HSF1's ablation in mice. HSF1 null mice showed increased brown (BAT) and inguinal fat depots (iWAT) (Figure 2A), enhanced lipid deposition (Figure 2B), decreased levels of brown fat markers (Figure 2C), and reduced UCP1 staining and levels in iWAT (Figures 2D and 2E). These alterations were associated with decreased total body oxygen consumption (Figure 2F), impaired cold resistance (Figure 2G), and reduced levels of *PGC1α* and *UCP1* in brown and inguinal fat tissue of cold-exposed HSF1 null mice (Figure 2H), with no concomitant changes in food intake nor in locomotor activity (Figures S2A and S2B). The impaired gene expression and metabolic responses observed in HSF1 null mice were recapitulated in isolated cells obtained from BAT and iWAT, showing reduced *PGC1α* and *UCP1* gene expression (Figure S2C) along with decreased oxygen consumption rates (OCRs) (Figure 2I), suggesting a cell-autonomous effect of HSF1's deletion on energetics. Taken together, these data demonstrate that HSF1's ablation in mice alters mitochondrial and brown fat gene programs in brown and inguinal fat tissues and affects thermogenic function and energy expenditure.

HSF1 Regulates White Fat Browning through PGC1α

Given the importance of inducible brown adipocytes in white fat (Harms and Seale, 2013), we next asked if modulation of HSF1's levels specifically in white fat depots could recapitulate, at least in part, the effects of HSF1's deficiency on brown and white fat observed in HSF1 null mice. Several methods have been recently used to study tissue- and depot-selective effects of gain or loss of function of specific genes circumventing the generation of conditional knockout mice (Kraus et al., 2014; Whittle et al., 2012; Qian et al., 2013). We took advantage of adenoviral delivery techniques we previously used to efficiently up- or downregulate genes of interest selectively in inguinal fat tissues of C57BL/6J mice (Ma et al., 2014). HSF1 depletion in iWAT was associated with increased size of subcutaneous fat cells, decreased UCP1 staining, and reduced levels of brown fat markers (Figures 3A–3D). Conversely, increased HSF1 expression in iWAT was associated with induction of browning, brown fat gene programs, and PGC1α and UCP1 protein levels (Figures 3E–3H). The delivery of shHSF1 and HSF1 adenoviruses appeared to be specific to iWAT, given that HSF1 levels were modulated only in this depot (Figures S3A and

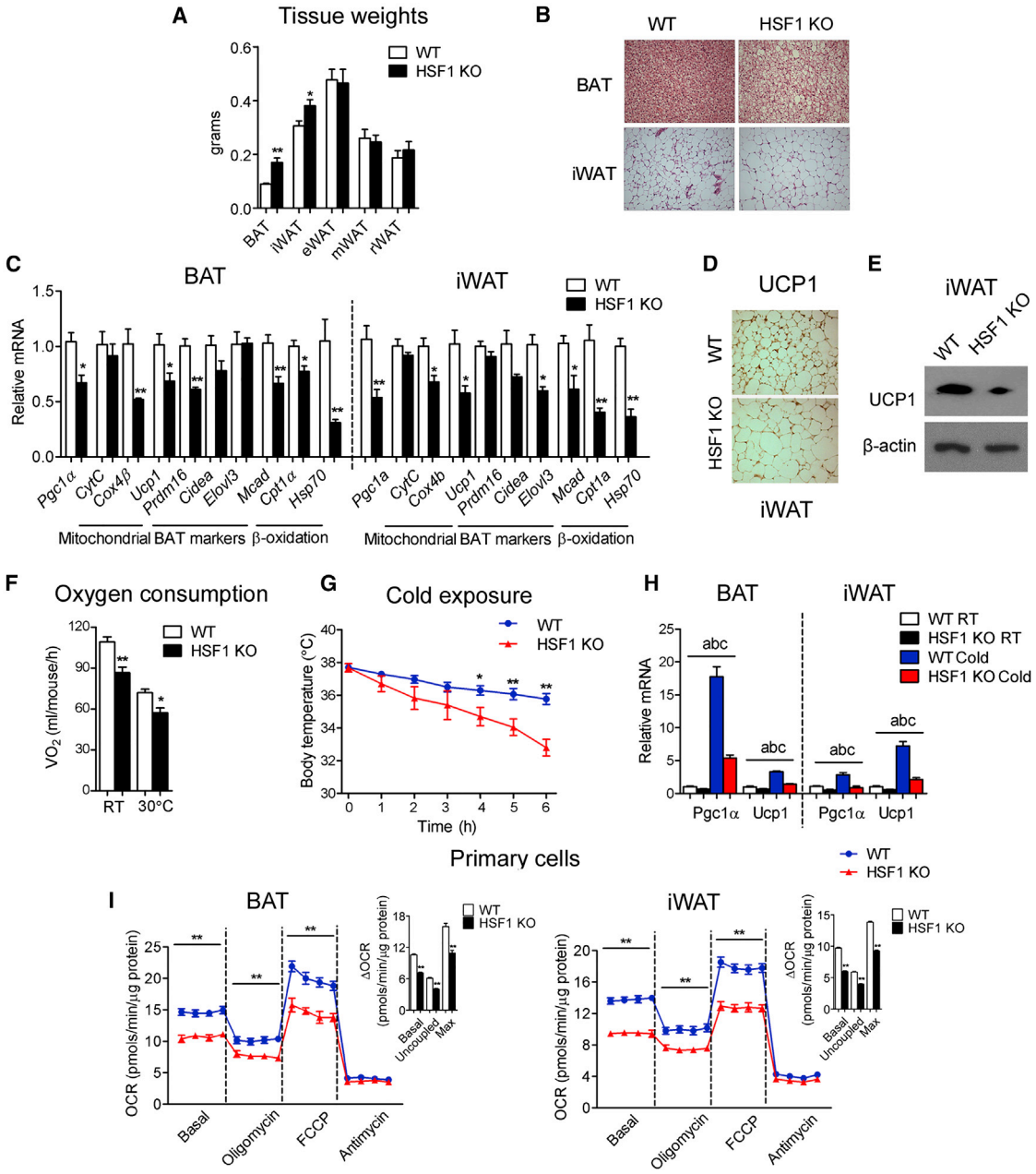

Figure 2. HSF1 Null Mice Have Impaired Energy Metabolism

(A–H) Analysis of 2-month-old WT and HSF1 null (HSF1 KO) mice.

(A) Weights of brown (BAT), inguinal (iWAT), epididymal (eWAT), mesenteric (mWAT), and retroperitoneal (rWAT) fat pads.

(B) Representative H&E staining of BAT and iWAT.

(C) Gene expression analysis of brown fat markers in BAT and iWAT.

(D and E) Representative UCP1 staining and UCP1 protein levels in iWAT.

(F) Oxygen consumption levels. ANCOVA analysis using body weight and genotype as covariance shows significant decrease in oxygen consumption in HSF1 null mice ($p = 0.018$ at room temperature and 0.046 at thermoneutrality, $n = 4$).

(G) Core temperatures during cold exposure.

(H) *PGC1α* and *UCP1* levels in BAT and iWAT obtained from mice at room temperature (RT) or after 6 hr of cold exposure (4°C). Annotation indicates significant effect of a, genotype; b, temperature; or c, significant temperature-genotype interaction using two-way ANOVA analysis.

(I) Oxygen consumption rate (OCR) in differentiated primary SVF cells from BAT and iWAT of 2-month-old WT and HSF1 null mice in basal conditions, in the presence of 1 μM oligomycin, 1 μM FCCP, or 0.5 μM Antimycin A. ΔOCR is calculated by subtracting OCR measured after antimycin addition from basal OCR, from OCR after oligomycin addition, or from OCR after FCCP addition.

$n = 6$ per group unless stated otherwise. Data are presented as mean ± SEM and $^*p < 0.05$, $^{**}p < 0.01$ compared to control group.

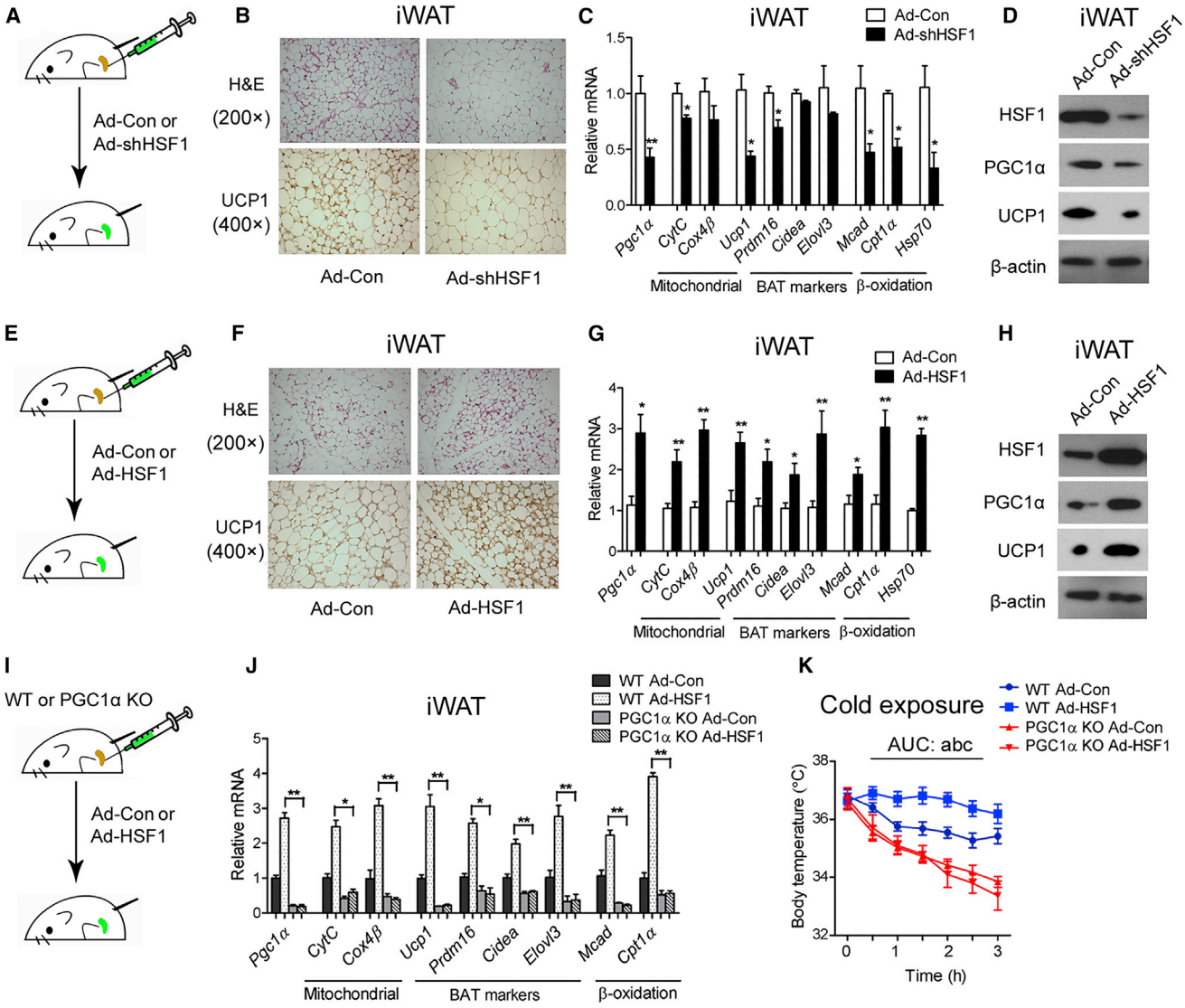

Figure 3. Modulation of HSF1 Levels in iWAT Affects Browning through PGC1α

(A) Schematic representation of the experimental design through (B)–(D).

(B–D) (B) Representative H&E and UCP1 staining; (C) mRNA levels of thermogenic and brown fat genes; and (D) protein levels of HSF1, PGC1α, and UCP1 in iWAT of 2-month-old mice injected with control (Ad-Con) or shHSF1 (Ad-shHSF1) adenovirus in iWAT depots.

(E) Schematic representation of the experimental design through (F)–(H).

(F)–(H) (F) Representative H&E and UCP1 staining; (G) mRNA levels of thermogenic and brown fat genes; and (H) protein levels of HSF1, PGC1α, and UCP1 in iWAT of 4-month-old mice injected with adenovirus expressing either control (Ad-Con) or HSF1 (Ad-HSF1).

(I) Illustration of the experimental design for the delivery of control or HSF1 adenoviruses into the iWAT of 4-month-old WT or PGC1α null (PGC1α KO) mice.

(J) mRNA levels of HSF1 and brown fat genes in iWAT obtained from WT and PGC1α null mice injected with control (Ad-Con) or HSF1 (Ad-HSF1) adenovirus.

(K) Core temperatures of WT and PGC1α null mice injected with control (Ad-Con) or HSF1 (Ad-HSF1) adenovirus during 3 hr of cold exposure. AUC (area under the curve) and annotation indicates significant effect of a, genotype; b, injection; or c, significant injection-genotype interaction using two-way ANOVA analysis.

n = 6 per group. Data are presented as mean ± SEM and *p < 0.05, **p < 0.01 compared to control group.

S3B). Overall these data further support a fat-cell-autonomous function of HSF1.

Given HSF1's ability to induce *PGC1α* and its downstream mitochondrial, brown fat, and energy utilization genes in vitro and in vivo (Figures 1–3), we next examined the requirement of *PGC1α* for HSF1-mediated regulation of these gene programs. As shown in Figures 3I–3K, ectopic expression of HSF1 in iWAT was associated with increased levels of mitochondrial and brown fat gene expression and improved cold tolerance in WT, but not in PGC1α KO mice. These results demonstrate that PGC1α is necessary for HSF1's metabolic action in inguinal fat tissues.

Celastrol Elicits Metabolic Effects through HSF1 and PGC1α

Having established the existence of the HSF1-PGC1α axis, we next tested whether pharmacological activation of this axis

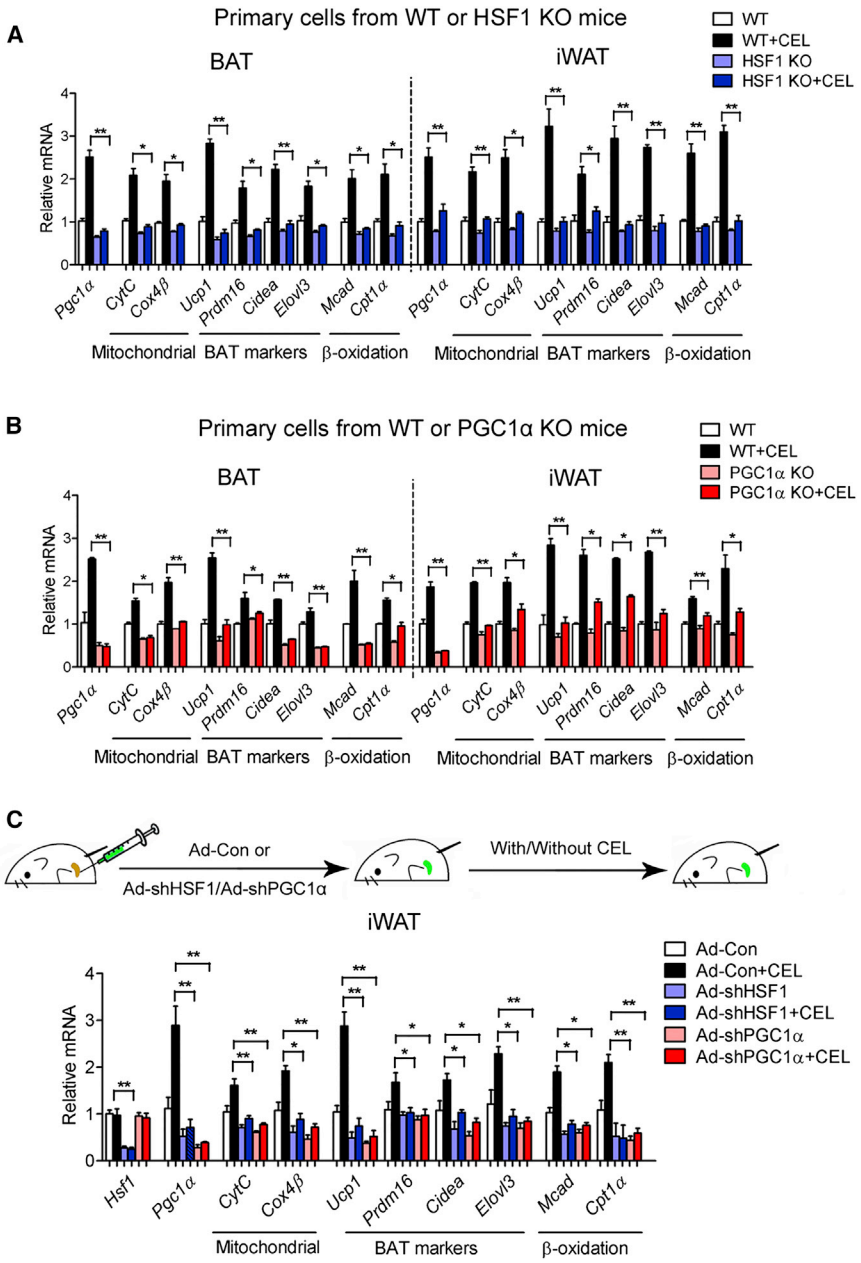

Figure 4. The HSF1 Activator Celastrol Elicits Metabolic Effects through HSF1 and PGC1α

(A and B) Gene expression analysis of mitochondrial and brown fat gene programs in differentiated primary cells (SVF) obtained from BAT and iWAT of 2-month-old WT, HSF1 null (HSF1 KO), or PGC1α null (PGC1α KO) mice, after treatment with vehicle or celastrol (CEL).

(C) mRNA levels of brown fat genes in inguinal fat tissue (iWAT) obtained from mice injected with either control (Ad-Con), shHSF1 (Ad-shHSF1), or shPGC1α (Ad-shPGC1α) adenoviruses and treated with or without CEL for 3 days. n = 6 per group. Data are presented as mean ± SEM and *p < 0.05, **p < 0.01, compared to control group.

in vivo would lead to enhanced brown fat functions. We chose to treat mice with the HSF1 activator celastrol, due to the clear in vitro effects of this compound on HSF1 and PGC1α (Figures 1A and 1C–1F), because of celastrol's known favorable safety profile in mice (Kiaei et al., 2005; Yang et al., 2006; Paris et al., 2010) and since our data suggested it has potent effects on primary human cells (Figure S1N). We first determined the specificity of celastrol's function and the genetic requirement of HSF1 and PGC1α for the celastrol-mediated activation of metabolic target genes. As shown in Figures 4A and 4B, the induction of thermogenic and mitochondrial gene programs elicited by celastrol in WT cells was markedly blunted in cells derived from either HSF1 or PGC1α null mice. To further determine whether the effects of celastrol were fat-cell-autonomous and dependent in vivo on the HSF1-PGC1α axis, we measured celastrol-mediated activation of metabolic genes in mice with HSF1 or PGC1α depletion selectively in iWAT and showed attenuated induction of mitochondrial, brown fat, and fatty acid utilization genes in response to treatment in the absence of either HSF1 or PGC1α (Figure 4C). Together, these data demonstrate that celastrol activates mitochondrial and thermogenic gene programs specifically through HSF1 and PGC1α.

HSF1 Activation by Celastrol Increases Energy Expenditure

Having demonstrated the specificity of the HSF1's activator celastrol, we next tested whether treatment of mice with this compound would lead to reprogramming of metabolic signatures in fat and other tissues. As shown in Figure 5A, the levels of *PGC1α* and of genes involved in brown fat and mitochondrial function, thermogenesis and lipid oxidation were increased in brown fat tissues of celastrol-treated mice, with no concomitant increase in adipogenic gene programs (Figure S4A). In addition, transmission electron microscopy (TEM) examination of BAT sampled from celastrol-treated animals showed increased mitochondrial number, as well as better preservation of mitochondrial cristae structure (Figure 5B), and molecular analysis demonstrated induction of classic markers of brown fat cells and beige cells (Figure 5C), increased UCP1 levels, and staining in iWAT (Figures 5D and 5E), with no effects on adipogenic gene programs (Figure S4A). Consistent with these molecular changes, celastrol-treated mice exhibited improved cold tolerance (Figure 5F). A similar induction of thermogenic and mitochondrial gene expression profiles (Figures S4B and S4C) and effects on browning (Figures S4D and S4E) were also observed in mice on chow diet treated with celastrol.

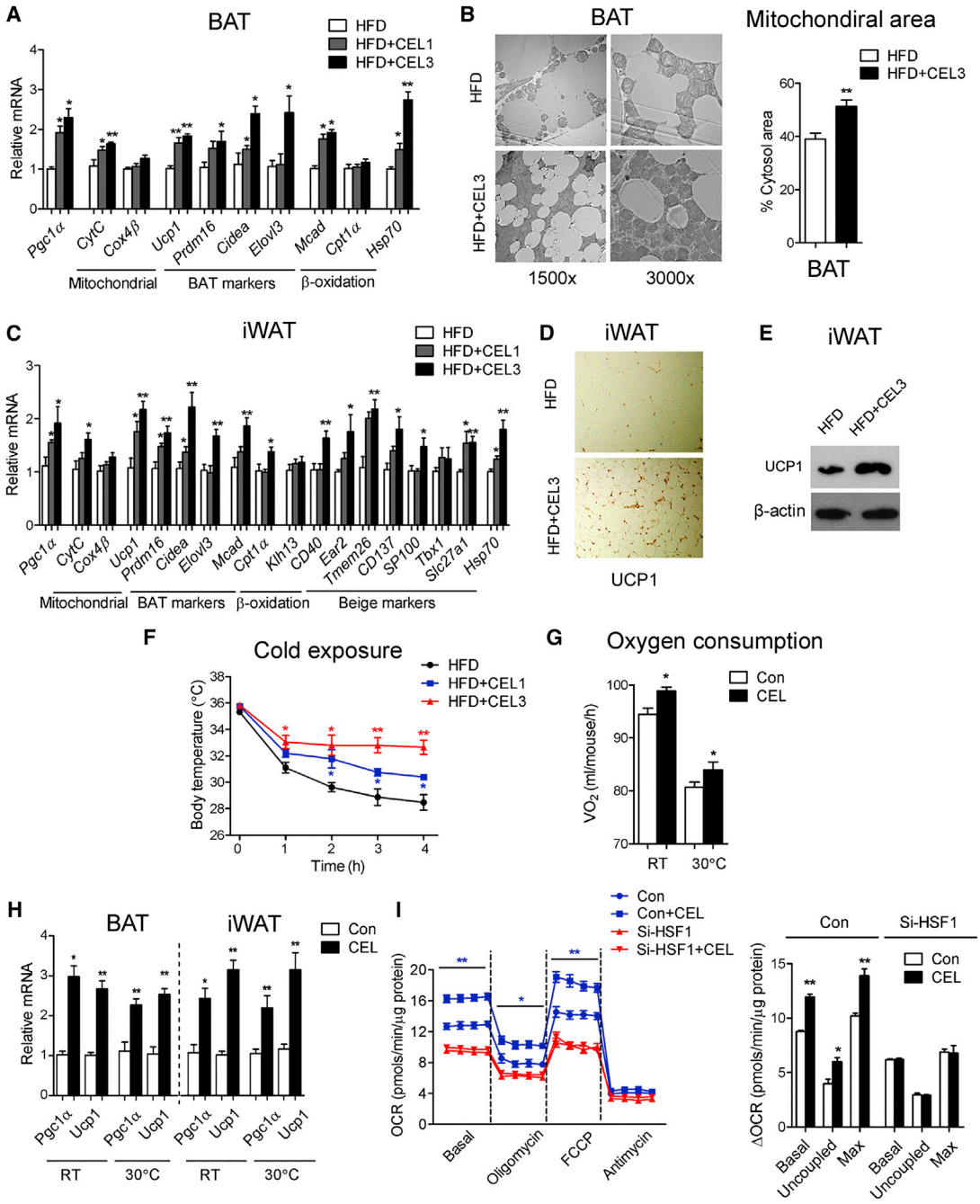

Figure 5. HSF1 Activation by Celastrol Induces Mitochondrial, Brown, and Beige Fat Programs in Adipose Tissues and Increases Energy Expenditure

(A–G) Analysis of mice on HFD, untreated (HFD, n = 6), or treated with celastrol at 1 mg/kg/day (HFD + CEL1, n = 6) or 3 mg/kg/day (HFD + CEL3, n = 7).

(A) Gene expression levels of brown fat programs in BAT.

(B) Representative transmission electron microscopy images (TEM) and quantification of mitochondrial area in BAT.

(C) Gene expression analysis of brown and beige selective genes in iWAT.

(D and E) Representative UCP1 staining and UCP1 protein levels of iWAT.

(F) Core body temperatures during cold exposure.

(G) Oxygen consumption levels and (H) *PGC1α* and *UCP1* levels in BAT and iWAT in mice treated with or without CEL for 3 days at room temperature (RT) or at thermoneutrality (30°C). n = 6.

(I) Oxygen consumption rate in differentiated 10T1/2 cells expressing control or siHSF1 in the presence of vehicle or 0.5 μM CEL for 72 hr, in basal conditions, or with 0.5 μM oligomycin, 1 μM FCCP, or 0.5 μM antimycin A. ΔOCR is calculated by subtracting OCR measured after antimycin addition from basal OCR, from OCR after oligomycin addition, or from OCR after FCCP addition.

Data are presented as mean ± SEM and *p < 0.05, **p < 0.01 compared to control group.

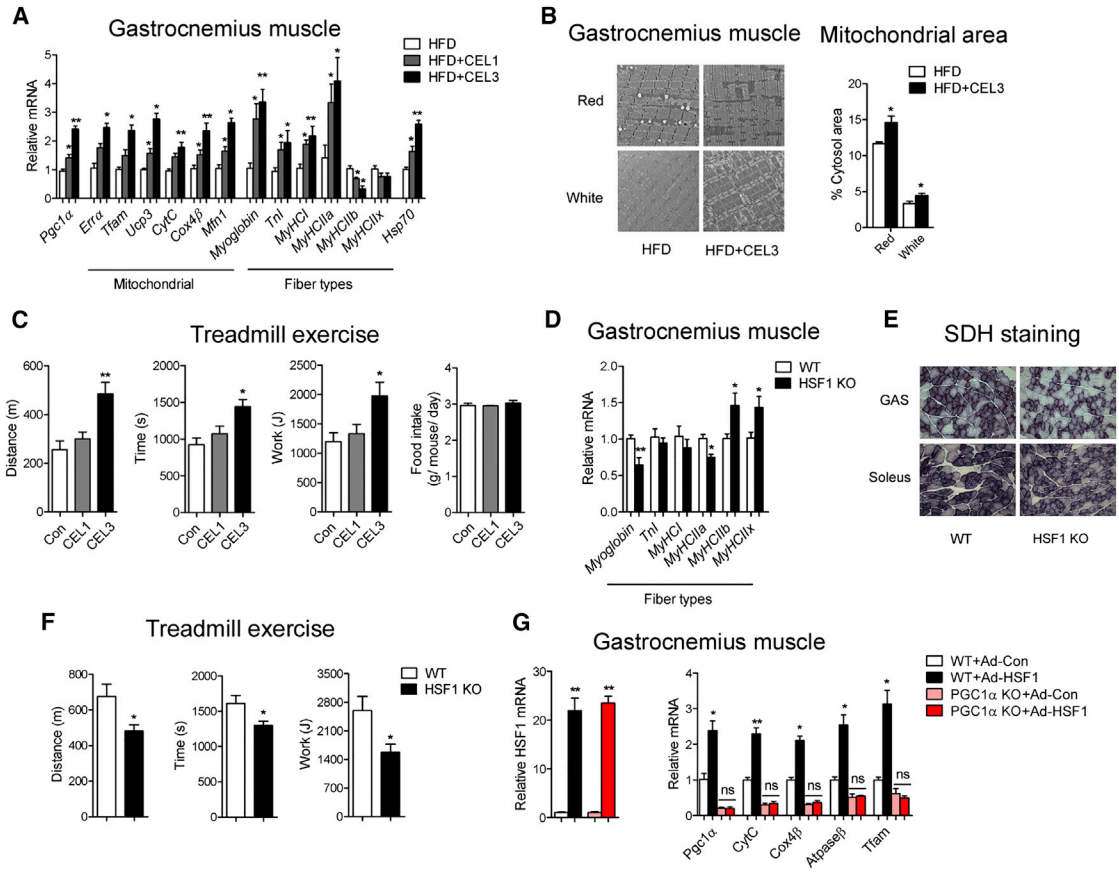

Figure 6. HSF1 Regulates Mitochondrial Function in Muscle

(A) Expression levels of *PGC1α* and of its downstream mitochondrial genes in the gastrocnemius of control and celastrol-treated mice (HFD, n = 6; HFD + CEL1, n = 6; HFD + CEL3, n = 7).

(B) Representative TEM image of red and white gastrocnemius muscle and quantification of mitochondrial areas.

(C) Exercise tolerance and food intake in mice treated with or without CEL for 10 days (n = 4).

(D) Expression of fiber type genes in the gastrocnemius muscle of 2-month-old WT and HSF1 KO mice (n = 6).

(E and F) SDH staining and treadmill performance of 2-month-old WT and HSF1 KO mice (n = 4).

(G) mRNA levels of *HSF1*, *PGC1α*, and mitochondrial genes in gastrocnemius muscle of 2-month-old WT and PGC1α KO mice injected with control (Ad-Con) or HSF1 (Ad-HSF1) adenovirus unilaterally into the contralateral lower limbs (n = 4 per group).

Data are presented as mean ± SEM and *p < 0.05, **p < 0.01 compared to control group.

We next determined the effects of pharmacological activation of HSF1 on energy expenditure and showed that administration of celastrol to mice housed at either room temperature or at thermoneutrality was associated with increased oxygen consumption and with elevation of brown fat gene expression programs in BAT and iWAT (Figures 5G and 5H), with no concomitant changes in food intake nor in locomotor activity (Figures S4F and S4G). The effects on oxygen consumption were recapitulated in vitro and abolished in HSF1-depleted cells, demonstrating that celastrol affects energy expenditure in a HSF1-dependent manner (Figure 5I).

Celastrol Increases Mitochondrial Function in Muscle

To determine whether the HSF1-PGC1α axis was also activated in other metabolic tissues in addition to fat, we analyzed the levels of PGC1α and its target genes in muscle, brain, kidney, and liver of celastrol-treated mice and in mice with HSF1 ablation (Figures S5A and S5B). This survey revealed that the transcriptional program downstream of PGC1α is activated also in skeletal muscle. Furthermore, we examined the expression of hypothalamic genes regulating energy balance previously reported to be altered in mice with neuronal specific knockout of PGC1α (Ma et al., 2010) and showed no changes in their expression levels in treated mice (Figure S5C).

Since it has been shown that PGC1α function in muscle contributes to energy expenditure (Handschin and Spiegelman, 2006; Lagouge et al., 2006), we further analyzed the effects of HSF1 activation on *PGC1α* and on its targets in mice treated with celastrol during HFD and demonstrated increased expression of mitochondrial and fiber-type genes (Figure 6A), reduced ectopic fat deposition (Figure 6B), and increased mitochondrial number in the gastrocnemius of celastrol-treated mice (Figure 6B). Given that modulation of PGC1α levels in muscle has been shown to affect exercise tolerance (Handschin et al., 2007), we tested the effects of celastrol treatment on muscle endurance. Our analysis revealed that treated mice had

increased ability to run longer, to cover a larger distance, and to generate higher average work compared to controls (Figure 6C), consistent with an overall increase in muscle endurance.

Conversely, mice with ablation of HSF1 showed reduced oxidative fibers in their gastrocnemius (Figures 6D and 6E) and impaired muscle endurance (Figure 6F). Furthermore, HSF1 gain of function in muscle was associated with increased expression of mitochondrial genes in WT but not in PGC1α KO mice, suggesting that the effects of HSF1 on muscle physiology are PGC1α dependent (Figure 6G). Overall, these data suggest a role of the HSF1-PGC1α axis also in modulating muscle physiology.

Celastrol Protects against Obesity, Insulin Resistance, and Hepatic Steatosis through HSF1 Activation

To further examine the physiological implications of the metabolic reprogramming induced by celastrol, we assessed whether HSF1 pharmacological activation would prevent obesity. As shown in Figure 7A, celastrol treatment throughout the HFD regimen protected mice from weight gain, without affecting their food intake, locomotor activity, or respiratory exchange ratio (Figure S6A). Examination of body composition by NMR spectroscopy revealed a marked and selective decrease in fat mass in celastrol-treated mice (Figures 7B and S6B). Consistent with this reduction, we observed decreased adipose depots exhibiting smaller adipocytes and reduced lipid accumulation (Figures 7C and 7D), an improvement in metabolic parameters (Figures 7E and S6B), and enhanced insulin sensitivity (Figures 7F) in the celastrol-treated group. Reductions in the liver enzyme alanine transaminase (ALT) and in the levels of the proinflammatory cytokine TNFα were also observed in the treated group (Figure S6C). Further evidence of improved metabolic profiles in celastrol-treated mice was the decrease in liver weights due to reduced hepatic steatosis and intrahepatic triglycerides accumulation (Figures 7G–7I). Interestingly, celastrol treatment of mice on regular chow diet also was associated with a reduction in adipose depots, but not with body weight changes (Figures S6D and S6E). To further ensure that the effects of celastrol on body weight were not related to compound toxicity, we monitored a number of parameters from the beginning of the treatment over a 2 week period. As shown in Figures S6F–S6J, while celastrol-treated mice showed decreased body weight and increased oxygen consumption compared to control mice, they had similar food intake and locomotor activity. Blinded analysis of H&E-stained histological tissue sections revealed no apparent pathology (Figure S6K), and serum chemistry analysis demonstrated the absence of any readily apparent drug toxicity (Table S1). As further evidence of the specificity of the compound and the genetic requirement of HSF1, celastrol treatment in HSF1 null mice had no effects on body weight, metabolic parameters, cold tolerance, or brown fat gene programs in BAT or iWAT (Figures 7J and S6L). Overall, these data demonstrate that pharmacological activation of HSF1 protects from diet-induced obesity and improves metabolic parameters in mice.

DISCUSSION

We have uncovered a critical role for HSF1 as a transcriptional regulator of brown fat, beige fat, and muscle physiology. HSF1 has been traditionally characterized as an ancient, conserved factor protecting cells against protein misfolding and aggregation induced by heat shock and shown to increase longevity in *C. elegans* by promoting protein homeostasis (Morley and Morimoto, 2004). Recently, HSF1 has been tied to negative outcomes in tumors by mediating the emergence of a stress-resistant phenotype in malignant cancers through activation of transcriptional programs principally involved in protein folding, mitosis, and translation (Mendillo et al., 2012). Our findings suggest that the role of HSF1 may need to be extended beyond its well-characterized role in chaperone protein regulation. The unsuspected and surprising role of HSF1 reported here suggests fundamental differences from that exerted in response to hyperthermia and in tumor cells, in that it directly drives the transcriptional activation of PGC1α-mediated gene programs required for adaptive energy metabolism. While our results show that HSF1-mediated "browning" of subcutaneous white fat tissue requires PGC1α, we cannot rule out that HSF1 may also exert its function through other regulators of beige fat tissue biology, such as via the transcriptional cofactor PRDM16 (Cohen et al., 2014), to orchestrate an inducible response to cold exposure. This possibility is consistent with our data showing HSF1-mediated PRDM16 mRNA regulation, both in isolated cells and in mouse tissues. A systematic genome-wide analysis of HSF1-activated transcriptional programs in fat tissues should provide further insights on the scope and scale of HSF1's role in brown and beige fat biology. Furthermore, our observation that HSF1 activation also elevated mitochondrial number and function in skeletal muscle suggests that the overall increased energy expenditure observed in celastrol-treated mice results from alterations in at least two distinct metabolically active tissues. Future analysis of the response of UCP1 KO mice to celastrol and of the extent of shivering of treated mice will help clarify the relative contribution of fat versus skeletal muscle in the HSF1-mediated metabolic effects elicited by celastrol.

The HSF1-regulated thermogenic gene program in white fat tissue can be recapitulated in isolated cells and appears to be sufficient to affect cellular respiration. Nonetheless, the presence of UCP1 does not always correlate with uncoupling activity; as such, further detailed analysis of this process in response to stimuli such as norepinephrine should provide a more detailed understanding of how HSF1 regulates thermogenic functions in brown and beige cells (Li et al., 2014). It has been recently shown that fat cells can sense cool temperatures directly, independently of the involvement of the canonical cAMP pathway or the TRPV family of thermosensors (Ye et al., 2013). Although it cannot be excluded that activation of the sympathetic nervous system during cold exposure may lead to activation of HSF1 in peripheral tissues, our data raise the possibility for a role of HSF1 in cold sensing and in switching on an intrinsic-thermogenic program in cells, suggesting a potential function of HSF1 as a stress response protein that may confer an "innate" ability of subcutaneous fat cells to initiate heat generation. Of note, the mechanisms for the activation of HSF1 via cold exposure are distinct from those elicited by hyperthermia and do not involve the hyperphosphorylation characteristic of heat-activated HSF1 (Cullen and Sarge, 1997). Whether cold stimuli induce distinct posttranslational modifications on HSF1 to affect its multimerization, changing its promoter binding patterns to include noncanonical binding motifs, and confer new gene target specificity needs to be further investigated.

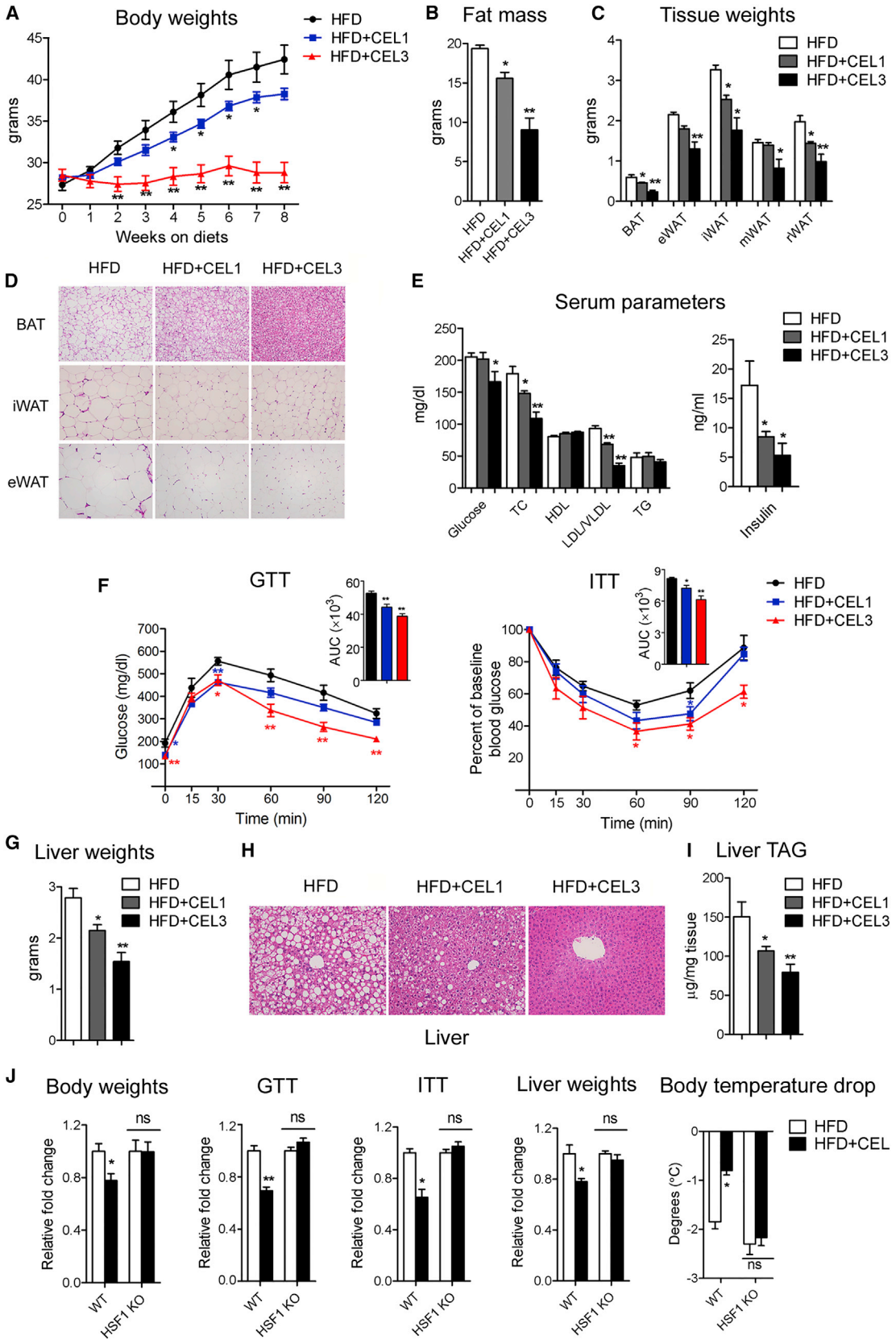

(legend on next page)

Our data suggest that pharmacological activation of the HSF1-PGC1α axis with celastrol ameliorates metabolic dysfunction. Of note, celastrol has been known for its antioxidative and anti-inflammatory properties (Salminen et al., 2010), and reported to cross the brain-blood barrier (Kiaei et al., 2005). Although our analysis did not reveal any significant changes in the levels of mitochondrial genes in the brain of treated mice, it remains to be assessed whether the beneficial effects of celastrol for the treatment of obesity are due to activation of the sympathetic nervous system in addition to its intrinsic effects on fat and muscle reported here.

Overall our study provides a proof of principle that pharmacological activation of HSF1 promotes thermogenic and mitochondrial gene programs in brown and beige cells and in skeletal muscle, with profound impact on metabolic parameters. The beneficial effects of HSF1 activation by celastrol observed in an animal model of diet-induced obesity included decreased adipose tissue expansion in response to HFD regimens and concomitant relief from the associated comorbidities, including improvement in insulin sensitivity and decreased hepatic steatosis. It is worth noting that, to date, pharmacological treatments such as those employing agonists for the β3-adrenergic receptor and for PPARγ have had little clinical success due either to their limited effects in enhancing energy expenditure (Cypess and Kahn, 2010; Cypess et al., 2012) or to dose-limiting adverse events (Boss and Farmer, 2012). In contrast, our data suggest that pharmacological activation of the HSF1-PGC1α axis may represent a possible strategy to ameliorate a wide range of pathologies associated with altered metabolic conditions.

While this paper was in revision, another report was published indicating that celastrol can act as a leptin sensitizer to counteract obesity (Liu et al., 2015). While both studies highlight the beneficial effects of celastrol in treating obesity, the two reports differ in the proposed mechanisms of celastrol's action. Specifically, the other recent report focused on celastrol's central effects on decreasing weight by affecting food intake, while our paper emphasizes celastrol peripheral action through activation of a transcriptional axis involving HSF1 and PGC1α. The contrasting mechanisms described in these two reports may reflect differences in the sensitivities of different tissues for different dosages of celastrol. This conclusion is bolstered by the fact that our analysis, using 3-fold fewer amounts of celastrol than recently described, did not uncover any effects on food intake. It should be noted that the two studies also differed on the models of obesity analyzed. Our studies involved normal mice fed a HFD, a condition in which celastrol was protective. In contrast, the other manuscript analyzed the effects of celastrol on obese and leptin-resistant mice. Interestingly, while the recent study primarily focused on celastrol effects on food intake, in their analysis they did observe that in pair-feeding experiments celastrol increased energy expenditure. Such results are consistent with our observations presented here. Further studies should help clarify whether central or peripheral effects of celastrol predominate at clinically relevant concentrations of the drug.

EXPERIMENTAL PROCEDURES

Cell Culture

10T1/2 cells (ATCC) and primary fat SVF cells were used in this study. A total of 90% confluent 10T1/2 cells were immediately transferred to a water bath placed inside a CO_2 incubator set at 37°C or 31°C for the indicated time. For heat shock experiments, 10T1/2 cells were exposed at 42°C for 1 hr. For cooling experiments, 10T1/2 cells were transfected with siRNA, and 48 hr later medium was changed with culture medium prewarmed at 37°C or 31°C and immediately transferred to a water bath placed inside a CO_2 incubator set at 37°C or 31°C for the indicated time. For the analysis of the effects of celastrol on gene expression of differentiated cells, 10T1/2 cells were treated with celastrol for 24 hr after 7 days of differentiation. The analysis of the effects of HSF1 knockdown was performed in 10T1/2 cells transfected with control or siHSF1 and differentiated for 4 days prior to treatment with 0.5 μM celastrol for 24 hr. To obtain WT, HSF1 null and PGC1α null mouse SVF, BAT, and iWAT were obtained from WT and null mice, minced, and subjected to collagenase (1 mg/ml) digestion at 37°C for 45 min in buffer containing 0.123 M NaCl, 5 mM KCl, 1.3 mM CaCl2, 5 mM glucose, 100 mM HEPES, and 4% BSA; filtered through a 100 um nylon screen; and centrifuged at 150 g for 5 min at room temperature. Cell pellets were washed twice and resuspended in DMEM medium containing 25 mM glucose, 20% FBS, 20 mM HEPES, and 1% pen/strep, and culture medium was changed daily. The differentiation process for 10T1/2 and SVF was described in Supplemental Experimental Procedures.

Cellular Metabolic Rates

Cellular metabolic rates were measured using a XF24 Analyzer (Seahorse Bioscience). 10T1/2 cells were transfected with control or si-HSF1 and differentiated for 5 days and/or treated with vehicle or celastrol for 72 hr. BAT and iWAT SVF cells from WT and HSF1 null mice were differentiated for 8 days. Respiration was measured under basal conditions, following the addition of ATP synthase inhibitor oligomycin, the mitochondrial uncoupler FCCP, or the complex III inhibitor antimycin A. The calculation methods can be found in Supplemental Experimental Procedures.

Transfections and Luciferase Assays

10T1/2 cells were transfected with Xtreme HP (Roche) or Nucleofector 96-well system (Amaxa). Gene expression analysis was performed 48 hr after transfection. Luciferase activity was assayed 24 hr after transfection with dual luciferase system (Promega). The PGC1α-luciferase reporter was purchased from Addgene. A deletion mutant of the PGC1α-luciferase reporter at the HSE putative sequence was generated with QuikChange II Site-Directed Mutagenesis Kit (Agilent), using the following primers: F, 5′-ATGTGCTGGGT TAGTTTTTTTAAAGTAGAATTAG-3′, and R, 5′-CTAATTCTACTTTAAAAAAAA CTAACCCAGCACAT-3′.

Real-Time PCR

Total RNA was extracted from cultured cells or tissues with TRIzol (Invitrogen), and 1 μg total RNA was reverse transcribed to cDNA with First-Strand cDNA Synthesis Kit (Roche), according to the manufacturers' instructions. Quantitative real-time PCR was performed with the ABI PRISM 7900HT sequence

Figure 7. HSF1 Activation Protects Mice from High-Fat-Diet-Induced Obesity, Insulin Resistance, and Hepatic Steatosis

(A–I) Analysis of mice on HFD, either without (HFD, n = 6) or treated with celastrol at doses of 1 mg/kg/day (HFD+CEL1, n = 6) or 3 mg/kg/day (HFD + CEL3, n = 7), including: (A) body weights; (B) fat mass; (C) weights of brown (BAT), inguinal (iWAT), epididymal (eWAT), mesenteric (mWAT), and retroperitoneal (rWAT) fat depots; (D) representative H&E staining of fat depots; (E) serum parameters; (F) GTT and ITT assays; (G) liver weights; (H) representative H&E staining of livers; and (I) intrahepatic triglyceride levels (TAG).

(J) Comparison between the response to CEL in 2-month-old WT and HSF1 KO mice on HFD supplemented with or without 3 mg/kg/day CEL for 4 weeks (n = 4 per group), including body weights, insulin sensitivity measured by GTT (AUC) and ITT (AUC), liver weights, and core temperatures during 4 hr of cold exposure. AUC, area under the curve. Data are presented as mean ± SEM and *$p < 0.05$, **$p < 0.01$ compared to control group.

detection system (ABI) using SYBR green (Roche). The details can be found in Supplemental Experimental Procedures.

Coimmunoprecipitation Assay and Protein Analysis

Coimmunoprecipitation was performed with the Catch and Release v2.0 Reversible Immunoprecipitation System (Millipore). Proteins were separated by 10% Bis-Tris Gel (Invitrogen), transferred to PVDF membranes (Pierce), and incubated with anti-PGC1α (Santa Cruz, sc-13067) or anti-HSF1 (Abgent, AJ1374a) antibodies overnight at 4°C and at room temperature for 1 hr with secondary antibodies. Immune complexes were visualized by using SuperSignal West Dura Extended Duration Substrate (Pierce), following the manufacturer's instructions. For measuring UCP1 protein levels in tissues with western blot analysis, proteins were extracted with RIPA buffer consisting of 20 mM Tris, 150 mM NaCl, 1% Triton X-100, and protease inhibitors (Roche), and 15 μg proteins were loaded on a 10% Bis-Tris Gel and transferred to PVDF membranes (Pierce) and incubated with anti-UCP1 (Abcam, ab10983) and anti-β-actin (Sigma, A5316) antibodies.

Chromatin Immunoprecipitation Assays

ChIP assays were performed using a ChIP assay kit (Millipore), according to manufacturer's instructions and as previous reported (Ma et al., 2014); details can be found in Supplemental Experimental Procedures.

Animal Studies

Mouse studies were performed according to guidelines of the National Institute of Diabetes and Digestive and Kidney Diseases Animal Care and Use Committee. C57BL/6J, HSF1 heterozygous mice (Balb/C) were purchased from The Jackson Laboratory. PGC1α heterozygous mice were a kind gift of Bruce M. Spiegelman (Harvard Medical School, Boston, MA, USA). Heterozygous mice were crossed to obtain WT and knockout genotypes. Male mice were used for all the experiments described in this study. For treatments, celastrol was mixed with powdered chow (NIH 07) or with HFD chow (60%, ResearchDiet, D12492). For assessing metabolic parameters, 2-month-old mice were fed either chow diet or HFD with or without celastrol for 3 weeks and 8 weeks. Body composition was measured using NMR (Echo Medical Systems). To monitor the effects of celastrol treatment, 2-month-old mice were fed HFD with or without celastrol for 2 weeks, and body weights, oxygen consumption, food intake and locomotor activity were measured every 2 days throughout the experiments with CLAMS (Columbus Instruments, Columbus, OH, USA). To measure the metabolic effects of celastrol on WT and HSF1 KO mice, 2-month-old mice were fed a HFD, with or without celastrol, for 4 weeks, and parameters such as body weight, insulin sensitivity, liver weights, and cold tolerance were measured at the end of the treatment. The details for cold exposure, treadmill exercise, energy expenditure, and GTT and ITT analysis can be found in Supplemental Experimental Procedures.

Adenoviral Delivery in Inguinal Fat and Muscle

Adenoviruses expressing control (CMV-GFP), mouse HSF1 (HSF1-CMV-GFP), control shRNA (U6-shRNA-CMV-GFP), shHSF1 (U6-shHSF1-CMV-GFP), and shPGC1α (U6-shPGC1α-CMV-GFP) were constructed, amplified, and purified by Vector Biolabs. A total of 50 μl of 5×10^9 Pfu of each adenovirus diluted in saline was injected bilaterally (s.c.) into the inguinal fat pads of mice (Ma et al., 2014). For intramuscular delivery of adenovirus, 10 μl of 2×10^{10} Pfu control or mouse HSF1 adenovirus diluted in saline was injected unilaterally into the contralateral lower limbs of mice (Ruas et al., 2012). Mice were either sacrificed at the fourth day after viral delivery or were celastrol treated as noted, and tissues were dissected for further analysis or monitored for changes in body temperature under cold environment for 3 hr.

Serum Parameters and Liver Triglyceride Level Determination

Serum leptin and insulin levels were measured with RIA kits (Millipore); blood glucose levels were measured with an automated reader (Bayer); triglyceride (Thermo), cholesterol (Sigma), HDL (Sigma), LDL/VLDL (Sigma), and ALT (Sigma) levels were assayed by colorimetric tests; and serum TNFα (R&D) and IFNγ (Phoenix Pharmaceuticals) were determined by ELISA. Analysis of serum chemistry including levels of serum minerals, lipids, and renal and liver enzymes was performed by the Department of Laboratory Medicine at the NIH Clinical Center. Lipids were extracted from liver samples, and triglyceride levels were determined by triglyceride reagent (Sigma). The details can be found in Supplemental Experimental Procedures.

Histological Analysis

Dissected tissues were fixed in 10% neutral buffered formalin and embedded in paraffin according to standard procedures. Tissue sections of 5 μm thickness were stained with H&E (Histoserv) or with UCP1 antibody (Abcam, ab10983), following the manufacturer's instructions (Vector labs). Frozen sections of gastrocnemius muscle from WT and HSF1 KO mice were prepared and stained with succinic dehydrogenase (SDH). Transmission electron microscopy (TEM) analysis was performed by EM Facility, National Cancer Institute, at Frederick, MD, USA. The details can be found in Supplemental Experimental Procedures.

Human Adipose Tissue

Fat biopsies of subcutaneous abdominal region were obtained from three obese women (BMI >40) recruited at the NIH. The study was approved by the NIDDK Institutional Review Board (clinicaltrials.gov identifier NCT00428987). All subjects gave written informed consent. SVF cells from human subcutaneous fat tissue were obtained, differentiated, and treated with DMSO or celastrol at the concentrations indicated for 24 hr. The details can be found in Supplemental Experimental Procedures.

Statistical Analysis

Student's t test was used for comparison between two groups. One-way ANOVA followed by the Dunnett post hoc test was used for multiple comparisons versus the control group (GraphPad Software). Two-way ANOVA was used to examine interactions between variables and ANCOVA was used to analyze oxygen consumption data of WT and HSF1 null mice by SPSS software (Tschöp et al., 2011). $p < 0.05$ was considered as statistically significant. Results are shown as mean ± SEM.

SUPPLEMENTAL INFORMATION

Supplemental Information includes six figures, one table, and Supplemental Experimental Procedures and can be found with this article at http://dx.doi.org/10.1016/j.cmet.2015.08.005.

AUTHOR CONTRIBUTIONS

X.M., L.X., and E.M. conceived the project. X.M. performed biochemical and cellular experiments, and L.X. performed animal experiments. A.T.A. performed the human primary adipocyte experiments. O.G. analyzed energy expenditure. A.B. performed preliminary experiments. M.S. recruited obese participants. J.L. assisted with measurement of cellular metabolic rates. T.F. participated in the experimental design and the interpretation of results. X.M., L.X., and E.M. wrote the manuscript. O.G. and T.F. edited the manuscript. E.M. devised the project, supervised, and coordinated the execution of the experimental plan.

ACKNOWLEDGMENTS

We are thankful to Richard Proia and Marc Reitman for reading the manuscript; to Pasha Sarraf for discussions throughout the project; and to Tatyana Chanturiya, Rachel Perron, and Ulrich Baxa for technical assistance. We also thank Jeffrey Kopp, Hidefumi Wakashin, and Shashi Shivrastav for kindly sharing their Seahorse Instrument; and Danielle Springer, Michele Allen, and Audrey Noguchi from the NHLBI murine core facility for technical support in metabolic phenotyping. This research was supported by funds of the NIDDK Intramural Research Program of the NIH.

Received: October 28, 2014
Revised: May 10, 2015
Accepted: August 5, 2015
Published: September 3, 2015

REFERENCES

Anckar, J., and Sistonen, L. (2011). Regulation of HSF1 function in the heat stress response: implications in aging and disease. Annu. Rev. Biochem. *80*, 1089–1115.

Bagattin, A., Hugendubler, L., and Mueller, E. (2010). Transcriptional coactivator PGC-1α promotes peroxisomal remodeling and biogenesis. Proc. Natl. Acad. Sci. USA *107*, 20376–20381.

Boss, O., and Farmer, S.R. (2012). Recruitment of brown adipose tissue as a therapy for obesity-associated diseases. Front. Endocrinol. (Lausanne) *3*, 14.

Bournat, J.C., and Brown, C.W. (2010). Mitochondrial dysfunction in obesity. Curr. Opin. Endocrinol. Diabetes Obes. *17*, 446–452.

Cantó, C., and Auwerx, J. (2009). PGC-1α, SIRT1 and AMPK, an energy sensing network that controls energy expenditure. Curr. Opin. Lipidol. *20*, 98–105.

Charos, A.E., Reed, B.D., Raha, D., Szekely, A.M., Weissman, S.M., and Snyder, M. (2012). A highly integrated and complex PPARGC1A transcription factor binding network in HepG2 cells. Genome Res. *22*, 1668–1679.

Cohen, P., Levy, J.D., Zhang, Y., Frontini, A., Kolodin, D.P., Svensson, K.J., Lo, J.C., Zeng, X., Ye, L., Khandekar, M.J., et al. (2014). Ablation of PRDM16 and beige adipose causes metabolic dysfunction and a subcutaneous to visceral fat switch. Cell *156*, 304–316.

Cullen, K.E., and Sarge, K.D. (1997). Characterization of hypothermia-induced cellular stress response in mouse tissues. J. Biol. Chem. *272*, 1742–1746.

Cunningham, J.T., Rodgers, J.T., Arlow, D.H., Vazquez, F., Mootha, V.K., and Puigserver, P. (2007). mTOR controls mitochondrial oxidative function through a YY1-PGC-1α transcriptional complex. Nature *450*, 736–740.

Cypess, A.M., and Kahn, C.R. (2010). Brown fat as a therapy for obesity and diabetes. Curr. Opin. Endocrinol. Diabetes Obes. *17*, 143–149.

Cypess, A.M., Lehman, S., Williams, G., Tal, I., Rodman, D., Goldfine, A.B., Kuo, F.C., Palmer, E.L., Tseng, Y.H., Doria, A., et al. (2009). Identification and importance of brown adipose tissue in adult humans. N. Engl. J. Med. *360*, 1509–1517.

Cypess, A.M., Chen, Y.C., Sze, C., Wang, K., English, J., Chan, O., Holman, A.R., Tal, I., Palmer, M.R., Kolodny, G.M., and Kahn, C.R. (2012). Cold but not sympathomimetics activates human brown adipose tissue in vivo. Proc. Natl. Acad. Sci. USA *109*, 10001–10005.

Eastmond, D.L., and Nelson, H.C. (2006). Genome-wide analysis reveals new roles for the activation domains of the Saccharomyces cerevisiae heat shock transcription factor (Hsf1) during the transient heat shock response. J. Biol. Chem. *281*, 32909–32921.

Egan, B., Carson, B.P., Garcia-Roves, P.M., Chibalin, A.V., Sarsfield, F.M., Barron, N., McCaffrey, N., Moyna, N.M., Zierath, J.R., and O'Gorman, D.J. (2010). Exercise intensity-dependent regulation of PGC1α mRNA abundance is associated with differential activation of upstream signalling kinases in human skeletal muscle. J. Physiol. *588*, 1779–1790.

Farmer, S.R. (2008). Molecular determinants of brown adipocyte formation and function. Genes Dev. *22*, 1269–1275.

Fujikake, N., Nagai, Y., Popiel, H.A., Okamoto, Y., Yamaguchi, M., and Toda, T. (2008). Heat shock transcription factor 1-activating compounds suppress polyglutamine-induced neurodegeneration through induction of multiple molecular chaperones. J. Biol. Chem. *283*, 26188–26197.

Gesta, S., Tseng, Y.H., and Kahn, C.R. (2007). Developmental origin of fat: tracking obesity to its source. Cell *131*, 242–256.

Guo, L., Chen, S., Liu, K., Liu, Y., Ni, L., Zhang, K., and Zhang, L. (2008). Isolation of heat shock factor HsfA1a-binding sites in vivo revealed variations of heat shock elements in Arabidopsis thaliana. Plant Cell Physiol. *49*, 1306–1315.

Handschin, C., and Spiegelman, B.M. (2006). Peroxisome proliferator-activated receptor γ coactivator 1 coactivators, energy homeostasis, and metabolism. Endocr. Rev. *27*, 728–735.

Handschin, C., Rhee, J., Lin, J., Tarr, P.T., and Spiegelman, B.M. (2003). An autoregulatory loop controls peroxisome proliferator-activated receptor γ coactivator 1α expression in muscle. Proc. Natl. Acad. Sci. USA *100*, 7111–7116.

Handschin, C., Kobayashi, Y.M., Chin, S., Seale, P., Campbell, K.P., and Spiegelman, B.M. (2007). PGC-1α regulates the neuromuscular junction program and ameliorates Duchenne muscular dystrophy. Genes Dev. *21*, 770–783.

Harms, M., and Seale, P. (2013). Brown and beige fat: development, function and therapeutic potential. Nat. Med. *19*, 1252–1263.

Kiaei, M., Kipiani, K., Petri, S., Chen, J., Calingasan, N.Y., and Beal, M.F. (2005). Celastrol blocks neuronal cell death and extends life in transgenic mouse model of amyotrophic lateral sclerosis. Neurodegener. Dis. *2*, 246–254.

Kleiner, S., Mepani, R.J., Laznik, D., Ye, L., Jurczak, M.J., Jornayvaz, F.R., Estall, J.L., Chatterjee Bhowmick, D., Shulman, G.I., and Spiegelman, B.M. (2012). Development of insulin resistance in mice lacking PGC-1α in adipose tissues. Proc. Natl. Acad. Sci. USA *109*, 9635–9640.

Kraus, D., Yang, Q., Kong, D., Banks, A.S., Zhang, L., Rodgers, J.T., Pirinen, E., Pulinilkunnil, T.C., Gong, F., Wang, Y.C., et al. (2014). Nicotinamide N-methyltransferase knockdown protects against diet-induced obesity. Nature *508*, 258–262.

Lagouge, M., Argmann, C., Gerhart-Hines, Z., Meziane, H., Lerin, C., Daussin, F., Messadeq, N., Milne, J., Lambert, P., Elliott, P., et al. (2006). Resveratrol improves mitochondrial function and protects against metabolic disease by activating SIRT1 and PGC-1α. Cell *127*, 1109–1122.

Leone, T.C., Lehman, J.J., Finck, B.N., Schaeffer, P.J., Wende, A.R., Boudina, S., Courtois, M., Wozniak, D.F., Sambandam, N., Bernal-Mizrachi, C., et al. (2005). PGC-1α deficiency causes multi-system energy metabolic derangements: muscle dysfunction, abnormal weight control and hepatic steatosis. PLoS Biol. *3*, e101.

Lerin, C., Rodgers, J.T., Kalume, D.E., Kim, S.H., Pandey, A., and Puigserver, P. (2006). GCN5 acetyltransferase complex controls glucose metabolism through transcriptional repression of PGC-1α. Cell Metab. *3*, 429–438.

Li, Y., Fromme, T., Schweizer, S., Schöttl, T., and Klingenspor, M. (2014). Taking control over intracellular fatty acid levels is essential for the analysis of thermogenic function in cultured primary brown and brite/beige adipocytes. EMBO Rep. *15*, 1069–1076.

Lin, J., Wu, H., Tarr, P.T., Zhang, C.Y., Wu, Z., Boss, O., Michael, L.F., Puigserver, P., Isotani, E., Olson, E.N., et al. (2002). Transcriptional co-activator PGC-1 α drives the formation of slow-twitch muscle fibres. Nature *418*, 797–801.

Lin, J., Wu, P.H., Tarr, P.T., Lindenberg, K.S., St-Pierre, J., Zhang, C.Y., Mootha, V.K., Jäger, S., Vianna, C.R., Reznick, R.M., et al. (2004). Defects in adaptive energy metabolism with CNS-linked hyperactivity in PGC-1α null mice. Cell *119*, 121–135.

Liu, J., Lee, J., Salazar Hernandez, M.A., Mazitschek, R., and Ozcan, U. (2015). Treatment of obesity with celastrol. Cell *161*, 999–1011.

Long, J.Z., Svensson, K.J., Tsai, L., Zeng, X., Roh, H.C., Kong, X., Rao, R.R., Lou, J., Lokurkar, I., Baur, W., et al. (2014). A smooth muscle-like origin for beige adipocytes. Cell Metab. *19*, 810–820.

Ma, D., Li, S., Lucas, E.K., Cowell, R.M., and Lin, J.D. (2010). Neuronal inactivation of PGC-1α protects mice from diet-induced obesity and leads to degenerative lesions. J. Biol. Chem. *285*, 39087–39095.

Ma, X., Xu, L., Gavrilova, O., and Mueller, E. (2014). Role of forkhead box protein A3 in age-associated metabolic decline. Proc. Natl. Acad. Sci. USA *111*, 14289–14294.

Mendillo, M.L., Santagata, S., Koeva, M., Bell, G.W., Hu, R., Tamimi, R.M., Fraenkel, E., Ince, T.A., Whitesell, L., and Lindquist, S. (2012). HSF1 drives a transcriptional program distinct from heat shock to support highly malignant human cancers. Cell *150*, 549–562.

Morley, J.F., and Morimoto, R.I. (2004). Regulation of longevity in Caenorhabditis elegans by heat shock factor and molecular chaperones. Mol. Biol. Cell *15*, 657–664.

Mueller, E. (2014). Understanding the variegation of fat: novel regulators of adipocyte differentiation and fat tissue biology. Biochim. Biophys. Acta *1842*, 352–357.

Nedergaard, J., and Cannon, B. (2014). The browning of white adipose tissue: some burning issues. Cell Metab. *20*, 396–407.

Ouellet, V., Labbé, S.M., Blondin, D.P., Phoenix, S., Guérin, B., Haman, F., Turcotte, E.E., Richard, D., and Carpentier, A.C. (2012). Brown adipose tissue oxidative metabolism contributes to energy expenditure during acute cold exposure in humans. J. Clin. Invest. *122*, 545–552.

Paris, D., Ganey, N.J., Laporte, V., Patel, N.S., Beaulieu-Abdelahad, D., Bachmeier, C., March, A., Ait-Ghezala, G., and Mullan, M.J. (2010). Reduction of beta-amyloid pathology by celastrol in a transgenic mouse model of Alzheimer's disease. J. Neuroinflammation *7*, 17.

Patti, M.E., and Corvera, S. (2010). The role of mitochondria in the pathogenesis of type 2 diabetes. Endocr. Rev. *31*, 364–395.

Qian, S.W., Tang, Y., Li, X., Liu, Y., Zhang, Y.Y., Huang, H.Y., Xue, R.D., Yu, H.Y., Guo, L., Gao, H.D., et al. (2013). BMP4-mediated brown fat-like changes in white adipose tissue alter glucose and energy homeostasis. Proc. Natl. Acad. Sci. USA *110*, E798–E807.

Reinke, H., Saini, C., Fleury-Olela, F., Dibner, C., Benjamin, I.J., and Schibler, U. (2008). Differential display of DNA-binding proteins reveals heat-shock factor 1 as a circadian transcription factor. Genes Dev. *22*, 331–345.

Ruas, J.L., White, J.P., Rao, R.R., Kleiner, S., Brannan, K.T., Harrison, B.C., Greene, N.P., Wu, J., Estall, J.L., Irving, B.A., et al. (2012). A PGC-1α isoform induced by resistance training regulates skeletal muscle hypertrophy. Cell *151*, 1319–1331.

Salminen, A., Lehtonen, M., Paimela, T., and Kaarniranta, K. (2010). Celastrol: Molecular targets of Thunder God Vine. Biochem. Biophys. Res. Commun. *394*, 439–442.

Sharp, L.Z., Shinoda, K., Ohno, H., Scheel, D.W., Tomoda, E., Ruiz, L., Hu, H., Wang, L., Pavlova, Z., Gilsanz, V., and Kajimura, S. (2012). Human BAT possesses molecular signatures that resemble beige/brite cells. PLoS ONE *7*, e49452.

Skarulis, M.C., Celi, F.S., Mueller, E., Zemskova, M., Malek, R., Hugendubler, L., Cochran, C., Solomon, J., Chen, C., and Gorden, P. (2010). Thyroid hormone induced brown adipose tissue and amelioration of diabetes in a patient with extreme insulin resistance. J. Clin. Endocrinol. Metab. *95*, 256–262.

St-Pierre, J., Drori, S., Uldry, M., Silvaggi, J.M., Rhee, J., Jäger, S., Handschin, C., Zheng, K., Lin, J., Yang, W., et al. (2006). Suppression of reactive oxygen species and neurodegeneration by the PGC-1 transcriptional coactivators. Cell *127*, 397–408.

Tschöp, M.H., Speakman, J.R., Arch, J.R., Auwerx, J., Brüning, J.C., Chan, L., Eckel, R.H., Farese, R.V., Jr., Galgani, J.E., Hambly, C., et al. (2011). A guide to analysis of mouse energy metabolism. Nat. Methods *9*, 57–63.

Westerheide, S.D., Bosman, J.D., Mbadugha, B.N., Kawahara, T.L., Matsumoto, G., Kim, S., Gu, W., Devlin, J.P., Silverman, R.B., and Morimoto, R.I. (2004). Celastrols as inducers of the heat shock response and cytoprotection. J. Biol. Chem. *279*, 56053–56060.

Whittle, A.J., Carobbio, S., Martins, L., Slawik, M., Hondares, E., Vázquez, M.J., Morgan, D., Csikasz, R.I., Gallego, R., Rodriguez-Cuenca, S., et al. (2012). BMP8B increases brown adipose tissue thermogenesis through both central and peripheral actions. Cell *149*, 871–885.

Wu, Z., Puigserver, P., Andersson, U., Zhang, C., Adelmant, G., Mootha, V., Troy, A., Cinti, S., Lowell, B., Scarpulla, R.C., and Spiegelman, B.M. (1999). Mechanisms controlling mitochondrial biogenesis and respiration through the thermogenic coactivator PGC-1. Cell *98*, 115–124.

Wu, J., Boström, P., Sparks, L.M., Ye, L., Choi, J.H., Giang, A.H., Khandekar, M., Virtanen, K.A., Nuutila, P., Schaart, G., et al. (2012). Beige adipocytes are a distinct type of thermogenic fat cell in mouse and human. Cell *150*, 366–376.

Xu, Y.M., Huang, D.Y., Chiu, J.F., and Lau, A.T. (2012). Post-translational modification of human heat shock factors and their functions: a recent update by proteomic approach. J. Proteome Res. *11*, 2625–2634.

Yang, H., Chen, D., Cui, Q.C., Yuan, X., and Dou, Q.P. (2006). Celastrol, a triterpene extracted from the Chinese "Thunder of God Vine," is a potent proteasome inhibitor and suppresses human prostate cancer growth in nude mice. Cancer Res. *66*, 4758–4765.

Ye, L., Wu, J., Cohen, P., Kazak, L., Khandekar, M.J., Jedrychowski, M.P., Zeng, X., Gygi, S.P., and Spiegelman, B.M. (2013). Fat cells directly sense temperature to activate thermogenesis. Proc. Natl. Acad. Sci. USA *110*, 12480–12485.